

## Monthly Mean Island Surface Winds in the Central Tropical Pacific and El Niño Events\*

D. E. HARRISON

*NOAA/Pacific Marine Environmental Laboratory, Seattle, WA 98115*

(Manuscript received 13 April 1987, in final form 9 June 1987)

### ABSTRACT

The monthly mean surface wind changes during recent ENSO events, as observed from 11 islands in the tropical Pacific, are described. Two different composite ENSO wind fields are evaluated and compared. The month-to-month wind changes during each event are also discussed.

The wind changes for each event between 1953 and 1980 except 1969 show several common features:

(i) Westerly anomalies appear first west of the date line and then at the date line sometime in summer (0) to fall (0), then intensify over the following several months. The anomalies are confined to within  $\pm 3^\circ$  of the equator during this stage.

(ii) In either November (0), December (0), or January (+1) there is an abrupt southward shift of the narrow band of westerly anomalies, so that the maximum anomaly is then at  $\sim 5^\circ$ S latitude at the date line, and nearly normal conditions prevail north of the equator.

(iii) Westerly anomalies are gone or greatly reduced one to two months after the southward shift.

The event-to-event variations are considerable, particularly prior to July (0) and after February (+1), so that composites show much reduced anomaly amplitude and much smaller month-to-month anomaly changes than are typical of any given event. The large amplitude months of the composites show similarities with a composite by Rasmusson and Carpenter, but a number of significant differences are identified. These findings, and their relationship to existing simple ideas concerning tropical Pacific coupled ocean-atmosphere interactions, are discussed.

### 1. Introduction

Our knowledge of the detailed evolution of the surface wind field before and during El Niño events is sketchy because of the limited amount of data available from the tropical Pacific. Because there is considerable variance in the zonal wind at periods of 4 to 30 days and in the meridional wind between 4 and 7 days, as well as at daily periods (Luther and Harrison, 1984), the sampling density afforded by merchant vessels (typically three to five observations per  $2^\circ$  latitude by  $10^\circ$  longitude region per month) is not adequate to determine accurate monthly mean winds. Fortunately, some of the wind changes that occur during El Niño events are so large that they show up in studies based on ship data (e.g., Wyrki and Meyers, 1975; Goldenberg and O'Brien, 1981; Barnett, 1983); monthly mean analyses have been widely used as forcing fields for hindcasts of El Niño events via ocean circulation models (e.g., Busalacchi and O'Brien, 1981).

However, detailed knowledge of the winds has been severely hampered by the limited dataset. Rasmusson and Carpenter (1982, hereafter RC), in their influential study, composited and smoothed the available data

over seasons for the post-1950 El Niño events in order to try to increase the signal-to-noise level. The RC composite field has often been taken as a paradigm for a "canonical" El Niño event, and has been used in efforts to validate numerical models for the study of El Niño mechanisms (e.g., Zebiak, 1982, 1985). With further study it has become clear that there are substantial event-to-event differences in the evolution of both SST and surface wind fields. Because the ocean-atmosphere coupling mechanisms are very likely nonlinear, it is important to learn as much as possible about the individual events as well as to compare these with the best possible composite event data; the physics of the averaged composite event may prove to be significantly different from the physics of the individual events.

In this paper various long time series of data from the 11 tropical Pacific islands listed in Table 1 will be used to describe the monthly mean wind changes and anomalous wind changes for the El Niño events between 1953 and 1980.<sup>1</sup> These time series provide excellent sampling in time (typically several observations per day) and have been prepared from handwritten observer sheets, copied at the New Zealand Meteorolo-

\* Contribution No. 834 from NOAA/Pacific Marine Environmental Laboratory.

<sup>1</sup> Unfortunately it has not yet been possible to extend the time series to include the 1982-83 event.

TABLE 1. Island wind observations.

Island	Location	Number of observations per day	Data coverage (mo/yr)
Arorae	3°S 177°E	6	7/54–1/55, 3/55–8/59, 2/60–12/80
Beru	1°S 176°E	4	1/49–6/51, 3/51–11/80
Butaritari	3°N 173°E	4	7/55–1/57, 4/57–2/58, 1/59–7/60, 9/60–10/60, 1/61–12/80
Canton	3°S 172°W	4	11/49–9/67
Funafuti	8°S 179°E	6	1/49–10/51, 4/52–5/52, 8/52–7/58, 9/58–9/72, 11/72–11/80
Majuro	7°N 171°E	6	2/55–7/60, 9/60–12/80
Nanumea	6°S 176°E	4	3/49–5/51, 4/52–9/53, 11/53–12/53, 5/54–10/57, 5/58–12/80
Niulakitu	11°S 180°	4	4/49–5/50, 7/51–9/56, 11/56–2/57, 4/57–11/79
Nui	7°S 177°E	4	3/49–2/51, 5/52–5/69, 7/69–12/80
Ocean	1°S 170°E	6	3/53–12/54, 2/55–1/69, 3/69–11/77, 6/78–11/80
Tarawa	1°N 173°E	4	1/49–7/51, 1/52–10/55, 1/56–12/80

logical Data Centre and keypunched in the United States. Although the geographical coverage provided by islands with good records is limited, the dataset offers an important new look at the wind changes associated with El Niño events, particularly near the date line in the tropical Pacific.

## 2. Definition of anomalous conditions

Studies like this one conventionally define anomalous conditions by subtracting climatological means from particular values, where climatological means are defined by averaging over all appropriate, available data. Thus, e.g., the February 1956 anomalous wind would be the difference between the February 1956 monthly average wind and the average wind based on all February data in the record. However, the wind records with the most prominent El Niño changes tend to exhibit either El Niño conditions or non-El Niño conditions; no “anti-El Niño” conditions are clear (see appendix). This motivated evaluating an alternative, non-El Niño (NEN), climatology to be compared with the conventional (CON) climatology. The particular years excluded from the NEN climatology are discussed in section 3 and include all years between 1953 and 1980 that have been classified as El Niño years to the author’s knowledge.

The NEN climatology, within 3° latitude of the equator and between August and January, shows stronger easterly winds than the CON climatology. Differences of  $> 1 \text{ m s}^{-1}$  are often found within this region and time of year. The largest differences are up to  $2 \text{ m s}^{-1}$  and are found very close to the equator and west of the date line in October, November and December. More than 5 degrees off of the equator the differences between NEN and CON values are generally very much less than  $1 \text{ m s}^{-1}$ . The comparison further supports the earlier statement that no strong anti-El Niño conditions exist in this dataset. Since the maximum anomalous wind values reported in RC occur during the period and in the region of maximum differences, and are themselves no greater than  $2 \text{ m s}^{-1}$ , these differences are noteworthy.

Anomaly fields defined relative to the NEN climatology show clearer spatial patterns and evolution in time than do anomalies defined relative to the CON climatology. Thus attention shall be concentrated on the former. When anomalous winds are quite large, there is little need to differentiate between climatologies, but some periods in which the anomalies are weak or are developing rapidly appear different relative to the different climatologies.

It is convenient to focus subsequent discussion on the line of islands near the date line extending from Majuro (7°N, 172°E) to Niulakita (12°S, 179°E). The climatological wind fields at these islands will be needed for future reference. Figure 1 presents the monthly mean climatological vector winds for the CON climatology (Fig. 1a), for the NEN climatology (Fig. 1b), and for the difference between the CON and NEN climatologies (Fig. 1c). The annual cycle north of the equator is of modest amplitude and primarily involves variation of the zonal wind. South of the equator both zonal and meridional components have annual variation of several meters per second.

## 3. Composite El Niño results

Although there are many differences between El Niño events (see section 4), compositing the events together offers a convenient way to begin our examination of the evolution of the winds and wind anomalies during El Niño periods. Following RC we composite the same calendar month from episode to episode. Because there is little unanimity of opinion concerning which periods to composite, we have evaluated two composites. The first consists of significant events, 1956–57, 1965–66, 1972–73, and 1976–77, while the second includes these and all other years that have been treated as El Niño years, 1953, 1963, and 1969. As noted above we focus on the line of islands extending from 7°N to 12°S near the date line and draw upon other data as needed.

Figure 2 shows the monthly mean significant event composite wind field, month by month, beginning in

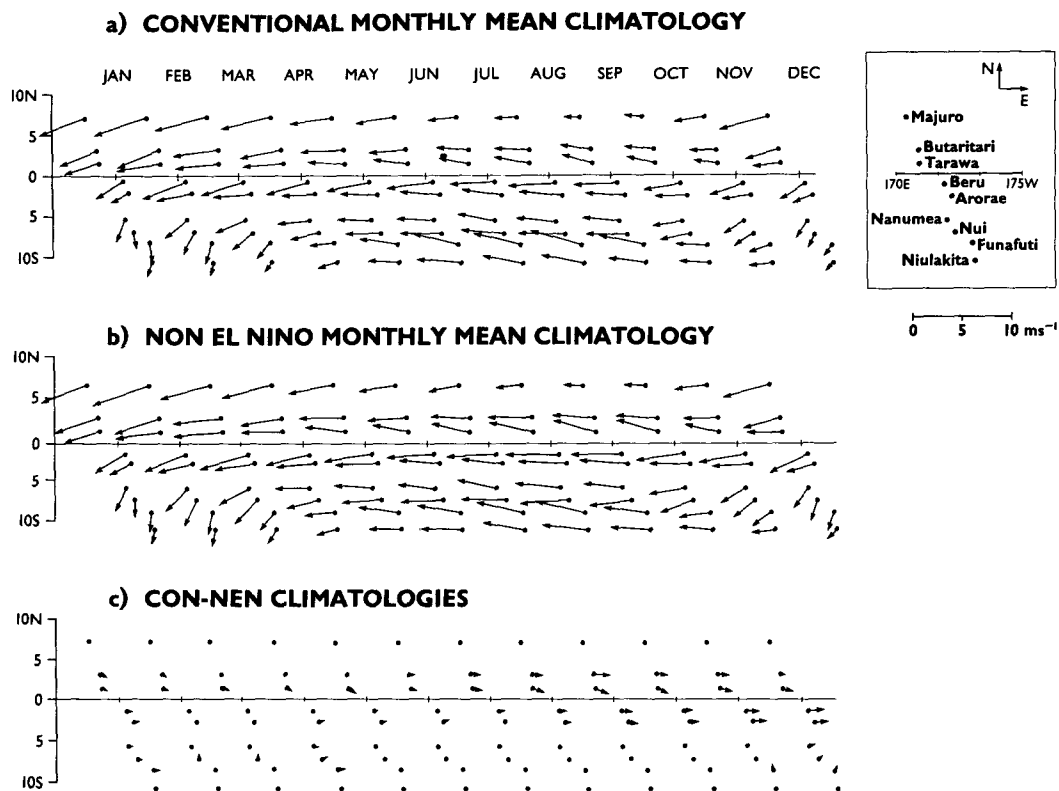


FIG. 1. (a) Conventional (CON) monthly mean climatological winds; (b) non-El Niño (NEN) monthly mean climatological winds; (c) difference between CON and NEN climatologies.

January (0), in the notation of RC. Prior to then (the start of the year in which South American coastal warming takes place) no clear signal is evident in the winds themselves. The composite is terminated in July (+1), because the El Niño signal is generally gone or dramatically diminished by that time. Simple visual comparison with the climatological cycle (Fig. 1) suggests that the first substantial departure from climatology occurs in May near the equator, as a weakening of the prevailing easterlies and a northerly deflection north of the equator. By July there is no wind at Butaritari (3°N) and half normal strength easterlies at Betio/Tarawa (1°N), but there is little change north or south of these islands. Through August, September, and October the weak equatorial easterlies are also noticed both north to Majuro (7°N) and south across the equator, but the weakening is more prominent north of the equator; actual westerly winds are found just north of the equator in September and October. Visible weakening of the prevailing easterlies at 5° and 6°S is seen by October. November brings weak westerly winds north and south of the equator and quite weak easterlies at 5° and 6°S.

A pronounced change in the wind pattern occurs in December, with a return to near-normal conditions north of the equator and now major disruption of the prevailing northeasterlies south of the equator. How-

ever, no westerly winds are found. In January (+1) the easterly wind component north of the equator is near normal, but the flow is more northerly; south of the equator the prevailing northeasterly (near equator) and northerly (5° to 12°S) winds are replaced with substantial northwesterly and westerly winds respectively. February (+1) brings another abrupt change, back toward climatological conditions at all locations. There continue to be weak departures from climatology, which decrease in amplitude with time, through March and April (+1). By May (+1) no departure from climatology is evident without careful scrutiny.

The smaller amplitude departures from climatology are much more easily seen by consideration of wind anomalies. Westerly anomalies are first seen at Ocean Island (170°E) in January and February (0) but are less than 2 m s<sup>-1</sup> (not shown). In the near date line data (Fig. 3), westerly anomalies first exceed 1 m s<sup>-1</sup> at all four near-equatorial islands in May (0), at which time the westerly anomaly at Ocean Island is stronger. The equatorial westerly anomalies increase in strength through the succeeding months; anomalies remain stronger at Ocean Island than near the date line, and stronger just north of the equator than just south of the equator near the date line until October (0). At that time the anomalies are of comparable strength near the date line and at Ocean Island. Westerly anomalies

**a) COMPOSITE EL NINO WINDS**

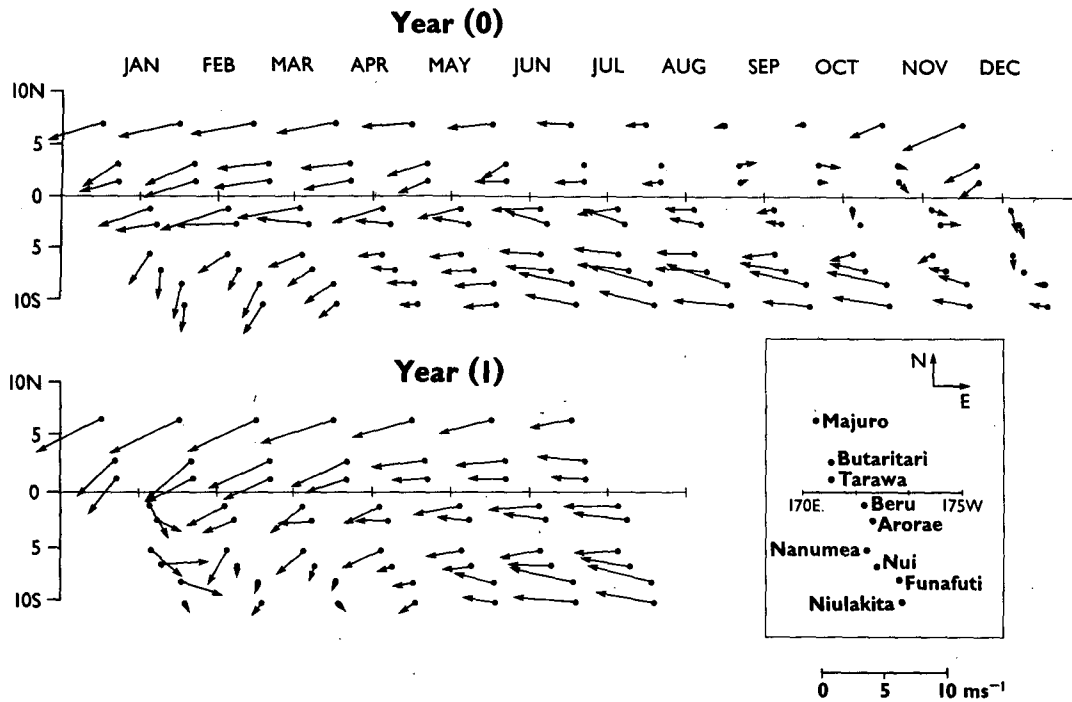


FIG. 2. Composite El Niño winds, based on all post-1953 El Niño periods.

**b) COMPOSITE EL NINO WIND ANOMALIES**

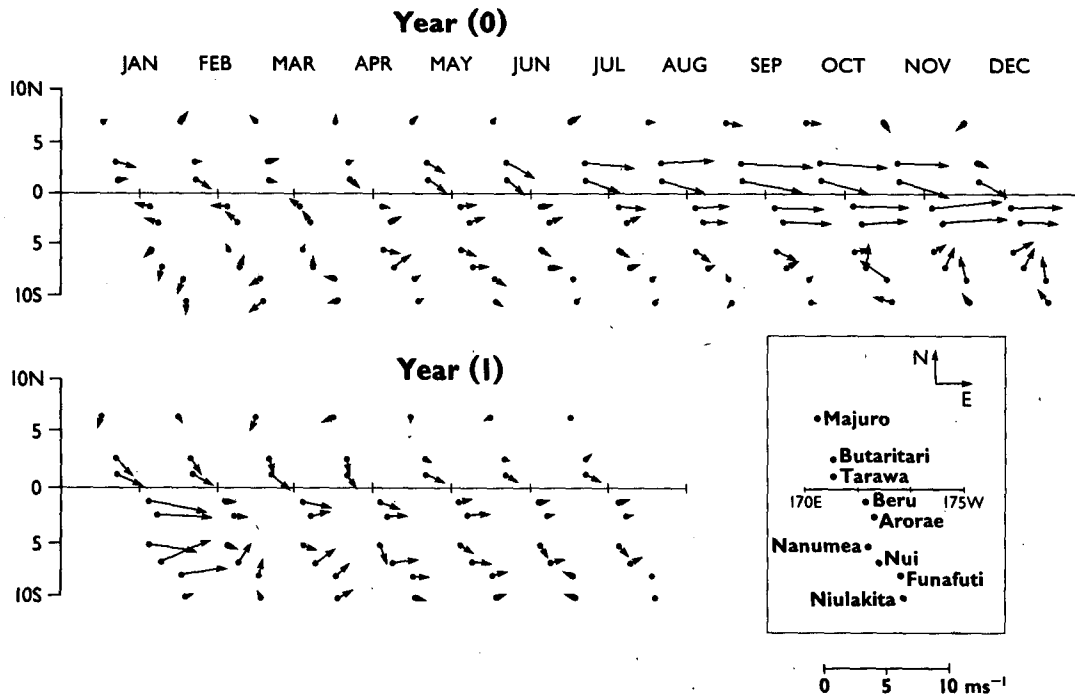


FIG. 3. Composite El Niño wind anomalies, based on subtracting NEN climatology from Fig. 2 composite.

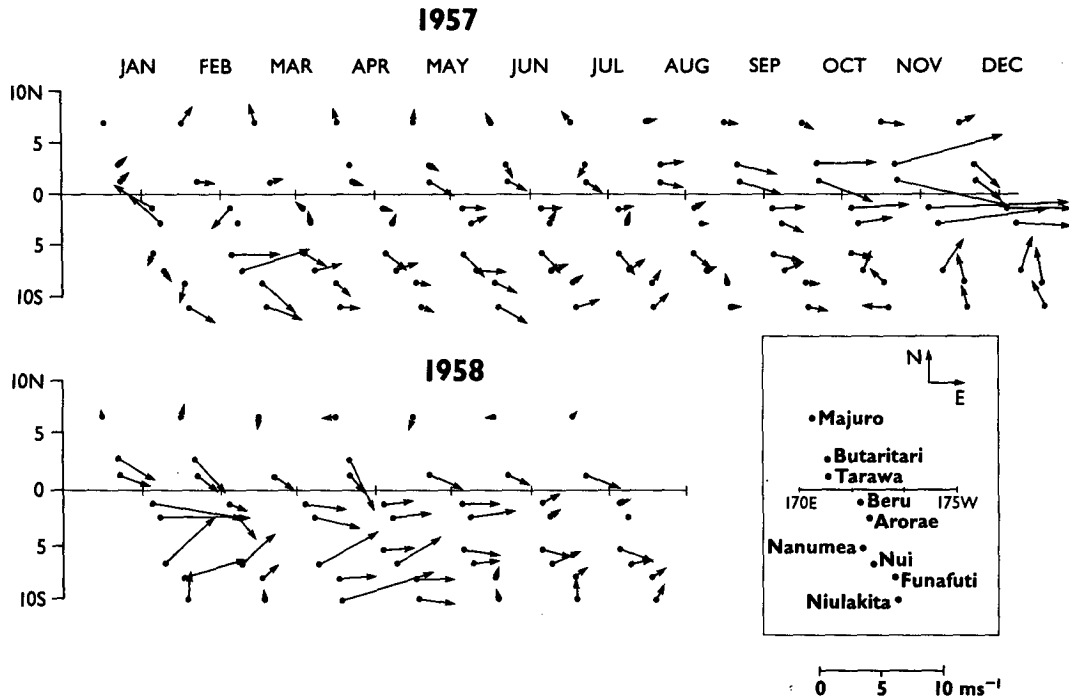


FIG. 4. Monthly mean wind anomalies for 1957-58 El Niño period.

at Canton (172°W) and Christmas (157°W) first appear in May (0), with the Canton anomaly larger than the Christmas anomaly. In June the anomalies at these islands are comparable, but are weaker than those of

the islands further west. Between August and October the amplitude of the westerly anomaly decreases eastward (from Ocean Island to date line to Canton to Christmas). In November the date line anomalies are

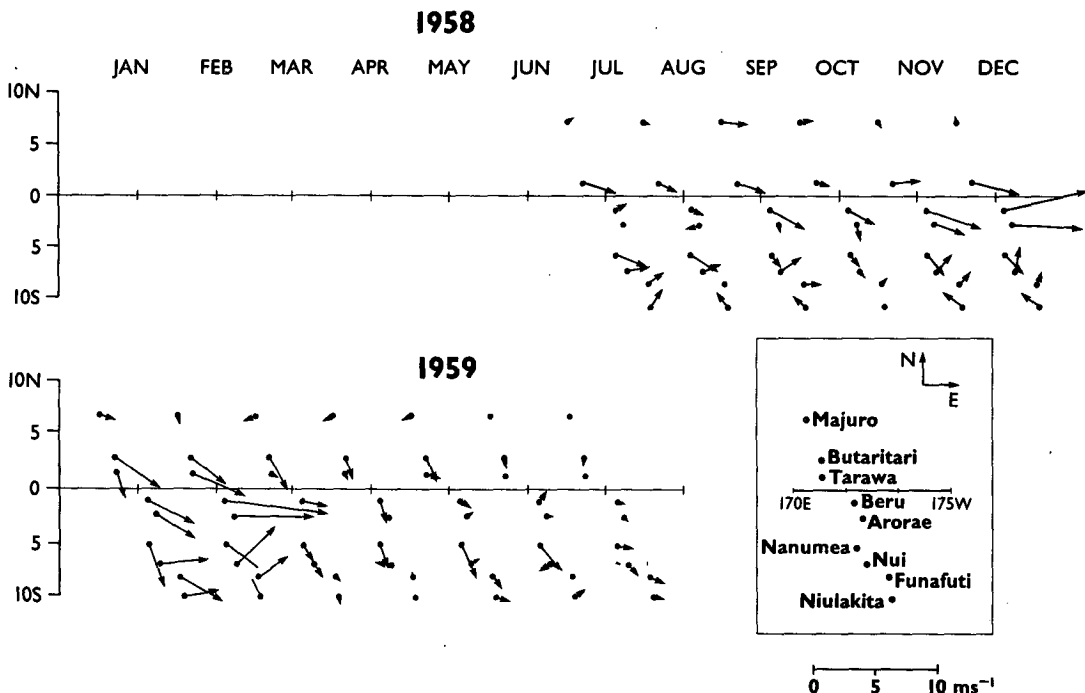


FIG. 5. As in Fig. 4 except for 1958-59 period.

the largest observed; greater than to the west at Ocean or to the east. The largest near equatorial anomaly,  $\sim 6 \text{ m s}^{-1}$ , occurs in November (0). December (0) brings a sharp reduction in the zonal anomaly at Ocean and just north of the equator near the date line, and an increase of westerly anomaly south of the equator and at Canton. In January (+1) the Canton anomaly is the largest found ( $\sim 6 \text{ m s}^{-1}$ ) and there is no strong westerly anomaly evident anywhere north of the equator. Westerly anomalies of as much as  $3 \text{ m s}^{-1}$  are, however, found as far south as  $10^{\circ}\text{S}$  at  $155^{\circ}\text{--}160^{\circ}\text{W}$ . February (+1) brings a sharp reduction of anomaly strength, to less than  $2 \text{ m s}^{-1}$  everywhere, and a less coherent anomaly pattern.

From the composite anomaly data, the very weak easterly winds at Majuro ( $7^{\circ}\text{N}$ ) in September and October (0) in Fig. 2 clearly are at least as much a reflection of the normal summer reduction of easterlies as the result of El Niño anomalous behavior; Majuro anomalies never exceed  $2 \text{ m s}^{-1}$ . Interestingly, there is no substantial, persistent westerly anomaly south of  $3^{\circ}\text{S}$ ; only December (0) and January (+1) show large signal of consistent direction.

The composite wind patterns near the date line for the second composite (not shown), incorporating the full group of El Niño years, is superficially similar to that of Fig. 2. However, the anomalous wind pattern for this second composite shows much smaller equatorial westerly anomalies; they do not exceed  $3 \text{ m s}^{-1}$  until August (0) and never exceed  $4 \text{ m s}^{-1}$ . The strongest anomaly seen in this composite is  $\sim 4.5 \text{ m s}^{-1}$  in January (+1), somewhat south of the equator. There is almost no anomaly poleward of  $3^{\circ}$  of the equator until year (+1), where westerlies are found, rather as in Fig. 3.

Relative to either climatology, the major features of the near date line composite anomaly pattern are clear. There are westerly anomalies confined closely to the equator ( $\sim 3^{\circ}$  latitude) which grow slowly between May (0) and September (0) north of the equator and between May and November just south of the equator. In December (0) and January (+1) the maximum anomaly shifts southward; in January (+1) the maximum anomaly is  $\sim 5^{\circ}\text{S}$  yet the pattern still has a meridional scale of  $\sim 3^{\circ}$ . After January (+1) the anomalies weaken sharply. No clear pattern is visible early in year (0) and no anomaly in excess of  $2 \text{ m s}^{-1}$  is found after April (+1).

Relative to the conventional climatology, the maximum anomaly amplitudes are smaller by up to  $\sim 2 \text{ m s}^{-1}$  and the patterns are considerably less clear. The summer (0)/fall (0) intensification appears much weaker and indicates that the anomalies increase from  $\sim 2 \text{ m s}^{-1}$  in July (0) to  $\sim 4 \text{ m s}^{-1}$  in October/November (0).

Some comparison of these composite results with those of Rasmusson and Carpenter (1982), whose results are based solely on ship reports, is of interest. The island results tend to support weak ( $\leq 1 \text{ m s}^{-1}$ ) easterly

anomalies near the date line in August–October (–1) as indicated by RC in their “antecedent” phase, but only relatively close to the equator, not with the considerable meridional extent indicated in RC’s Fig. 17. The island data show very little support for the RC near date line westerly anomalies during November (–1)–January (0). They also do not agree with the RC near date line anomalous northerlies between  $10^{\circ}\text{N}$  and the equator during March (0)–May (0), but agree somewhat (but only in the major events composite) concerning very weak westerly anomalies just south of the equator. For August (0)–October (0) near the date line both datasets show near-equatorial westerly anomalies, with maximum anomaly a little north of the equator, but the island data indicate much stronger equatorial anomalies. However, anomalies at  $7^{\circ}\text{N}$  are not comparable to those near the equator (as indicated in RC’s Fig. 20), and neither are there large scale southerly anomalies well south of the equator. For December (0)–February (+1) near the date line there is agreement that the maximum westerly anomalies are displaced a little south of the equator, but disagreement concerning the presence of comparably strong southerlies from  $10^{\circ}\text{S}$  to  $20^{\circ}\text{S}$  or between  $10^{\circ}\text{N}$  and  $3^{\circ}\text{N}$ .

Overall, then, these composite results differ in some nontrivial respects from those of RC. Several factors make direct comparison difficult. First, the island data come from regions in which RC had few ship data. One would therefore expect the RC composites to have less amplitude than that found in our well-sampled records, and to be subject to greater uncertainty than in other, better sampled, areas. Further, the ship data are very scattered in space and unevenly distributed in time. Rasmusson and Carpenter had no control over the data time distribution, which biases their composite toward the relatively well-sampled 1972 event, and adopted a spatial smoother to enable them to fill gaps and contour their fields. Here no spatial smoothing has been done and the date line data provide very good meridional coverage for these El Niño events. The considerable and consistent discrepancy in meridional scale of the near-equatorial anomalies may thus be a result of both the smoothing adopted and the bias toward the 1972 event (see next section). The off-equatorial northerly and southerly discrepancies may arise from the same factors; with the data at hand it simply is not possible to know. Unfortunately there are no instances available of a good near-equatorial island record in an area that is reasonably well sampled by ships; neither do these island records overlap in space or time with the records recently obtained from surface moored instruments. However, the consistency of independent observations from adjacent islands suggests that the island data are trustworthy in at least their larger signals.

#### 4. Individual El Niño events

We now turn to a brief look at the El Niño events that can be satisfactorily described by this dataset. As

before, it is convenient to concentrate on the behavior at the islands near the date line.

Figures 4 through 10 present monthly mean anomalous winds, relative to the NEN climatology for the 1957, 1963, 1965, 1969, 1972, and 1976 El Niño events. With the exception of 1969, each shares several common elements with the composite anomaly pattern—westerly anomalies appear quite near the equator (generally stronger just north of the equator) at some point in late Northern Hemisphere spring or summer, propagate eastward rapidly, intensify in strength and extend slowly southward over the next several months, then abruptly the whole pattern shifts somewhat south of the equator in December or January and then equally abruptly diminishes in strength in February. However, the timing of these changes and the strength of the anomaly during each phase varies considerably from event to event.

The 1957 event (Fig. 4) shows no systematic equatorial westerly anomalies early in the year, but has significant westerlies between  $5^{\circ}$  and  $11^{\circ}$ S from February through July. Westerlies first are seen at all four near-equatorial islands in May, but are not persistent until August and do not exceed  $3 \text{ m s}^{-1}$  until September ( $>5 \text{ m s}^{-1}$  first in November). Very strong near-equatorial anomalies (max  $\geq 11 \text{ m s}^{-1}$ ) exist in November 1957, and the southward anomaly shift takes place in December. Significant southerly anomalies exist between  $8^{\circ}$  and  $12^{\circ}$ S in November and December. Westerly anomalies persist south of the equator until May 1958, but are reduced to typically  $2 \text{ m s}^{-1}$  after April 1958. These late southern westerly anomalies are notable departures from most other events (in fact they largely account for the tendency toward weak westerlies in this area and period in the composite).

Although 1958 is not generally regarded as a separate El Niño event, it is interesting to compare its behavior between July 1958 and July 1959 (Fig. 5). There is no data at Butaritari ( $3^{\circ}$ N) until late December 1958. Comparison with the composite event shows many similarities—the evolution of the near-equatorial westerly anomalies in summer/fall 1958, the southerly flow in November and December 1958 south of  $6^{\circ}$ S, the southward shift of the westerly anomalies in January/February 1958 and the rapid diminution of the anomalies after February 1958. In terms of the wind anomalies, the post-July 1958 behavior can be treated as a distinct El Niño event, very similar to that of July 1957 to July 1958. If this interpretation is correct, it challenges the prevailing opinion that some period of time must elapse after a major collapse of the central Pacific trade winds (and the concomitant oceanic warming) before another El Niño event cycle can occur.

The 1963 event anomalies are presented in Fig. 6. Substantial easterly anomalies are found in January, February, and March, which is quite different from the composite and from other events. Westerly anomalies appear near the equator in June, but do not again appear at all four near-equatorial islands until September,

when the characteristic pattern of anomalies stronger just north of the equator is evident. The maximum equatorial westerly anomaly is  $\sim 6 \text{ m s}^{-1}$  in November and December. The shift south of the equator occurs in January 1964, and the anomalies are much reduced by February 1964. Easterly anomalies are typical after February 1964, in contrast to the weak westerly anomalies of the composite pattern.

In 1965 (Fig. 7) the early anomalies tend to be meridional rather than zonal at the date line but were westerly at Ocean Island in January and February. Then in June, westerly anomalies of up to  $4 \text{ m s}^{-1}$  abruptly appeared at the date line on both sides of the equator (they were present the month before at Ocean Island). These westerlies increased in strength through October, when the maximum anomaly was about  $8 \text{ m s}^{-1}$ . There was no clear shift of maximum anomaly strength from just north of the equator to just south of the equator, as in the composite, and the equatorial westerly anomalies abruptly diminished in December 1965, when there were strong SSE winds farther south. Then in January 1966, strong ( $9 \text{ m s}^{-1}$ ) westerly anomalies appeared somewhat south of the equator. By February 1966 there were no zonal anomalies greater than  $2 \text{ m s}^{-1}$ . Through the spring of 1966 there was an irregular tendency for weak westerly anomalies to exist.

In the 1972 event (Fig. 9) there are weak equatorial westerly anomalies in January, followed by generally easterly anomalies, quite strong ( $>5 \text{ m s}^{-1}$ ) south of the equator near the date line. March 1972 had only very weak anomalies throughout the western Pacific, but westerly anomalies of broad meridional scale appeared in May. These strengthened north of the equator, persisted just south of the equator, but basically disappeared further south in June 1972. Westerly anomalies returned at almost all latitudes, and with some strength ( $>5 \text{ m s}^{-1}$ ), just north of the equator in July 1972; they strengthened through August, September and October, to maximum near-equatorial values of  $\sim 9 \text{ m s}^{-1}$ . The southward shift occurred in November, a month ahead of the composite pattern, and the westerlies just south of the equator remained strong in December. Although they weakened somewhat in January 1973, the pattern stayed similar to that of December 1972. Westerly anomalies greater than  $5 \text{ m s}^{-1}$  were still present at  $7^{\circ}$ S in February 1973, again in contrast to the composite behavior. All significant anomalies are gone by March 1973 and none reappear subsequently.

The 1976 event (Fig. 10) had no significant near-equatorial anomalies until June, but there were north-easterly and then easterly anomalies south of the equator in January, February, and March. Near-equatorial westerly anomalies exceeded  $3 \text{ m s}^{-1}$  first in July but increased very little through August and September and never exceeded  $5 \text{ m s}^{-1}$ . In October and November the anomalies were very weak, but westerly anomalies appeared in the now-familiar pattern south of the equator in December, albeit with less amplitude than

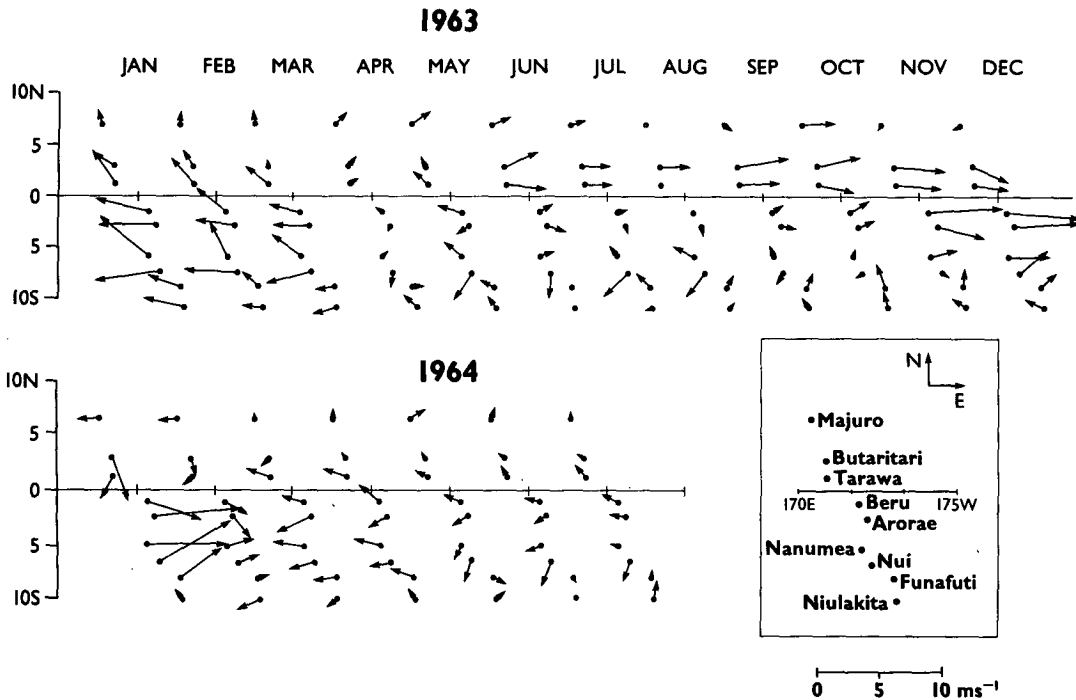


FIG. 6. As in Fig. 4 except for 1963–64 El Niño period.

is typical of other events (max  $\sim 3 \text{ m s}^{-1}$ ). January and February 1977 have only very weak and rather disorganized anomalies, while March 1977 has a return to westerly anomalies at most of the islands. However no pattern of intensification occurs later in 1977; weak

westerlies simply persist near the equator for several months.

The 1969 event (Fig. 10) is so different from these others that it has been saved for last. Through September, October and November 1968 there were equatorial

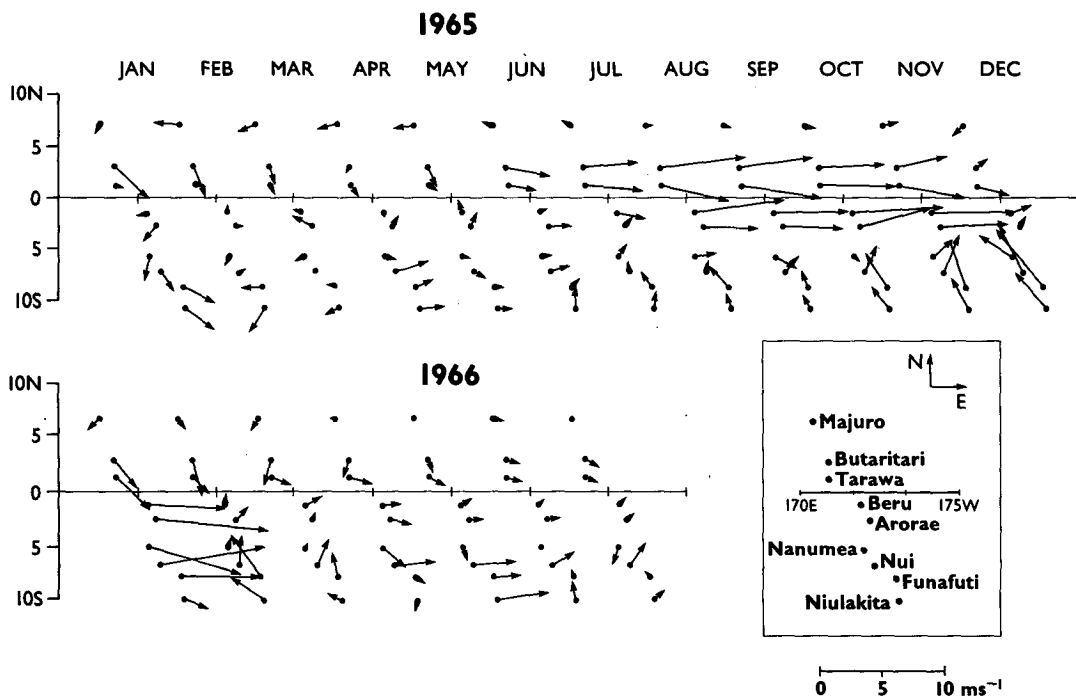


FIG. 7. As in Fig. 4 except for 1965–66 El Niño period.



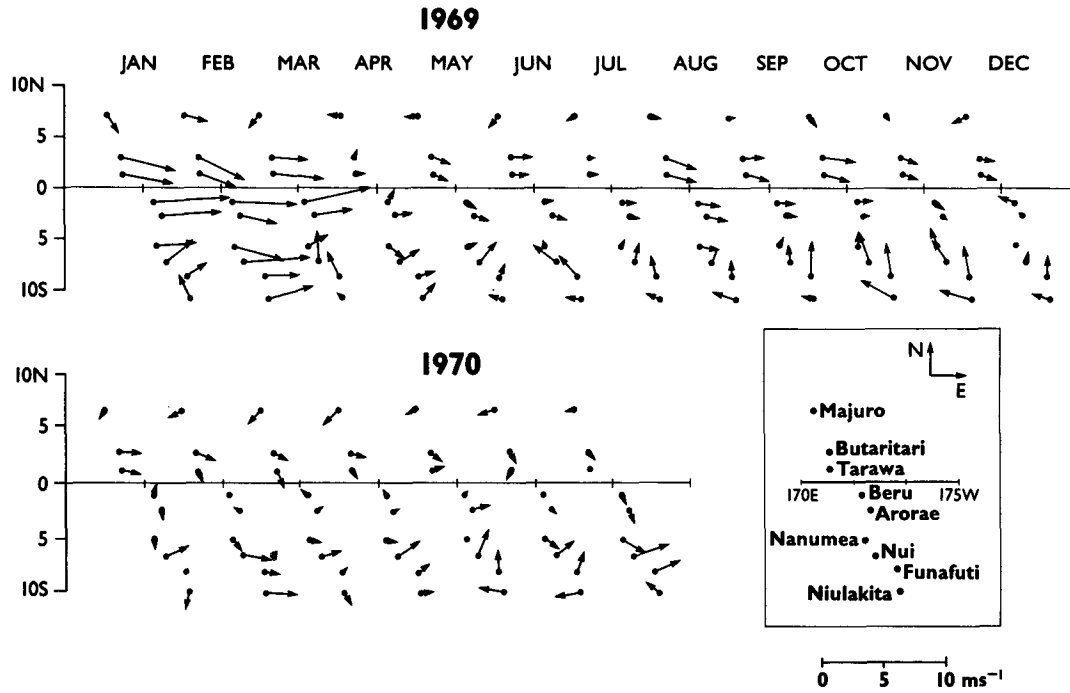


FIG. 8. As in Fig. 4 except for 1969-70 period.

westerly anomalies, typically of  $\sim 2 \text{ m s}^{-1}$ , but these vanished south of the equator in December 1968. Then strong westerly anomalies appeared in January 1969 (max  $\sim 7 \text{ m s}^{-1}$ ) and persisted through March near the equator. In April 1969 they abruptly diminished

in strength (to  $\leq 2 \text{ m s}^{-1}$ ), but these weak westerly anomalies persisted near the equator until December 1969. Typically there were southerly anomalies south of the equator through these last 9 months, but there was no consistent anomaly at  $7^\circ\text{N}$ . No late summer

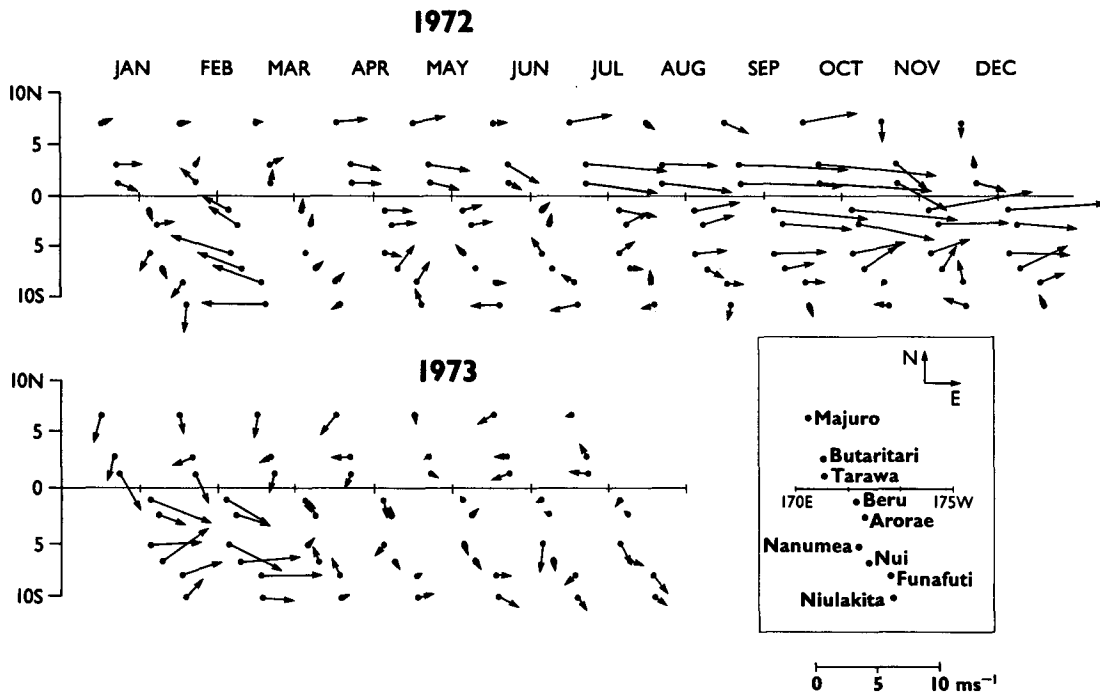


FIG. 9. As in Fig. 4 except for 1972-73 El Niño period.

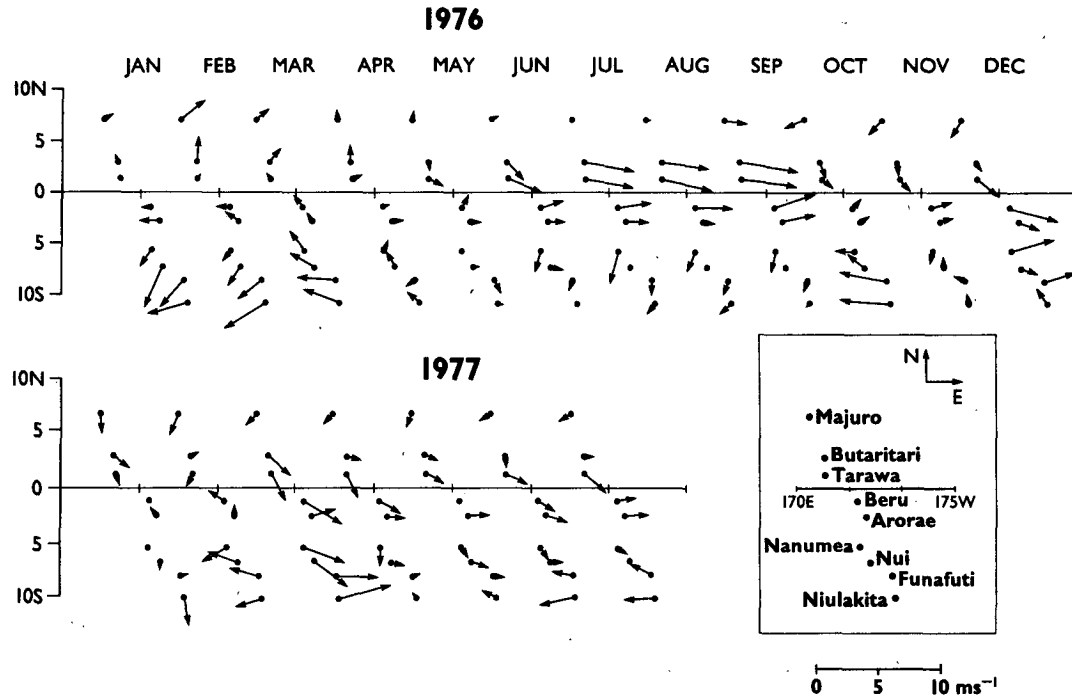


FIG. 10. As in Fig. 4 except for 1976–77 El Niño period.

or fall intensification occurred; neither was there a shift southward of anomaly pattern in December 1969 or January 1970. No systematic pattern of anomalies existed in 1970.

With the exception of the 1969 event, each event has the general features described earlier, but the timing within the year, the amplitude and the duration of each phase varies considerably from event to event (Table 2). In general, each event has larger amplitude anomalies than seen in the composite, as is to be expected given the event-to-event variations, and the composite gives the impression that the anomaly field evolves more slowly and systematically than is the case in particular events. As in our examination of the composite,

no evidence is observed for westward propagation or evolution of the equatorial wind anomalies—only progression from west to east is found. The fact that the two near-equatorial islands north of the equator are roughly seven degrees of longitude west of the southern near-equatorial islands, together with this eastern progression, may account for the observation that the equatorial westerly anomalies are initially greater north of the equator; Ocean Island, at 1°S and about 7° farther west of Butaritari, always has stronger westerly anomalies in the early stages than are found to the east and a little north. Figure 11 shows zonal wind anomalies for Ocean and Canton islands, for the events for which there is data at each island, to illustrate the phase

TABLE 2. El Niño event wind anomaly characteristics. See text for definition of anomaly used.

Event	Early equatorial easterlies/westerlies		Equatorial westerlies			Southward shift		Other
			>3 m s <sup>-1</sup>	>5 m s <sup>-1</sup>	maximum	time	maximum	
1957			Sep	Nov	11 m s <sup>-1</sup>	Dec, Jan	J, 7 m s <sup>-1</sup>	westerlies persist S of equator well into 1958
1958	N/A	N/A	Sep	Nov	7 m s <sup>-1</sup>	Jan, Feb	F, 9 m s <sup>-1</sup>	
1963	JFM		Jun	Nov	6 m s <sup>-1</sup>	Dec, Jan	J, 7 m s <sup>-1</sup>	westerlies weaken July, Aug 1963
1965			Jun	Aug	8 m s <sup>-1</sup>	J, 9 m s <sup>-1</sup>		
1969		JFM	Jan	Jan	7 m s <sup>-1</sup>			westerlies weaken after March 1969, never return with strength
1972	F	J	May	Jul	9 m s <sup>-1</sup>	Nov, Dec, Jan	N, 8 m s <sup>-1</sup>	westerlies weaken June 1972
1976			Jul		<5 m s <sup>-1</sup>	Dec	4 m s <sup>-1</sup>	westerlies weaken Oct, Nov 1976
Composite			Jul	Sep	6 m s <sup>-1</sup>	Dec, Jan	J, 5 m s <sup>-1</sup>	

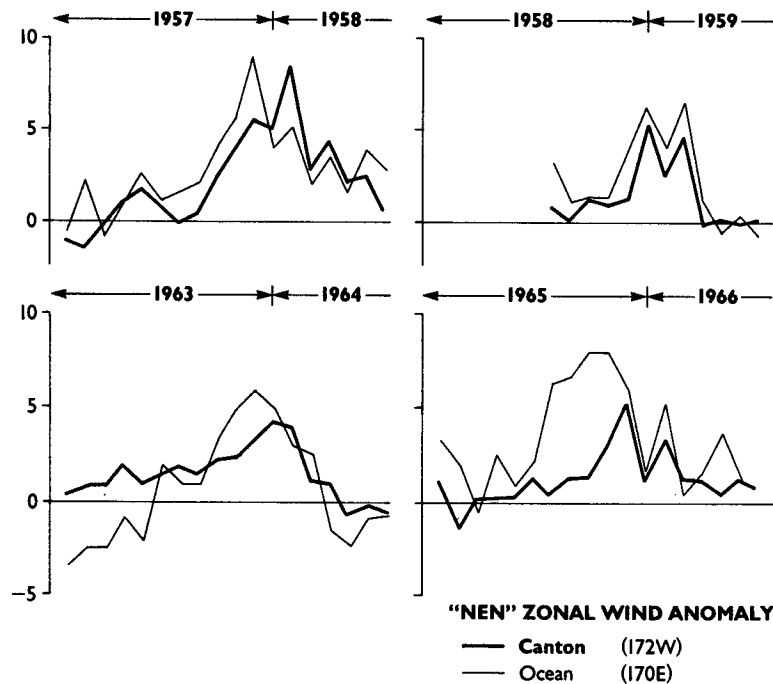


FIG. 11. Zonal wind anomalies at Canton (172°W) and Ocean (170°E), illustrating that central Pacific anomalies tend to develop later than more western Pacific anomalies.

lag between west and east of the date line. Recent results by Harrison and Gutzler (1986) and Gutzler and Harrison (1987) also show clear eastward wind anomaly progression; Barnett (1983) also suggested that eastward propagation is characteristic of his filtered low frequency surface wind anomalies.

## 5. Summary and discussion

We have examined the monthly mean wind and wind anomaly patterns of the central tropical Pacific, with particular attention to the changes that occur before and during El Niño events. Each event follows its own timing, but there are common phases of evolution between about July (0) and February (+1) except for the 1969 event. These common phases and their order of occurrence are

(i) The appearance of equatorially confined ( $\pm \sim 3^\circ$ ) westerly anomalies west of the date line and then near the date line, and their subsequent strengthening, with largest anomalies west of the date line [summer through fall, year (0)].

(ii) An eastward shift of the maximum equatorial westerly anomaly, from 170°E, to near the date line, and finally to  $\sim 170^\circ$ W [late in year (0)].

(iii) A southward shift of the westerly anomaly pattern, from roughly centered on the equator to centered  $\sim 5^\circ$ S [November (0), December (0) or January (+1)].

(iv) Rapid decrease of anomaly strength to  $\leq 2 \text{ m s}^{-1}$  at all islands sampled [February (+1) or March (+1)].

Phase (iii) may be separated from phase (ii) by as much as two months of weak anomalies, and phase (i) does not always follow the first appearance of equatorial westerly anomalies. Some evidence exists for weak equatorial easterly anomalies sometime between September (-1) and December (-1), but the timing and magnitude are quite variable. There is typically very little systematic signal in the anomaly field before June (0), or apart from the phases listed above. In particular, no clear evidence is found for persistent systematic anomalies off the equator.

One may wonder at the use of monthly means for this study, fearing contamination by 40 to 60 day variability; however there is not much power in these periods in the surface wind (a sharp contrast to the situation in the upper air) and aliasing does not appear a factor in this study. No filtering beyond monthly averaging has been done to these data, yet month-to-month evolution is quite clear and systematic.

The clear and systematic signals seen also strongly suggest that local island topographic effects and variable observer skills are not serious error sources in the data, at least on these time scales. The near-equatorial island data show great consistency in amplitude and timing, despite the fact that there is great day-to-day wind variability during ENSO events and that each record is independently obtained. Lacking high-quality local surface marine data it is not possible to calibrate the island data quantitatively, but the island-to-island consistency suggests that these amplitudes are not likely to be grossly in error.

The behavior of the composite anomaly pattern close to the equator and south of the equator in December (0) and January (+1) is just a smoothed-over average of the different events (excepting 1969). The composite amplitudes are considerably reduced from those typical of each event and the composite anomalies appear to evolve much more slowly because of the difference in phase timing between events. Off the equator the composite anomalies tend to be misleading, because strong anomalies in one event have significantly affected the composite, which is based on only a few events.

A limited comparison with the seasonally averaged Rasmusson and Carpenter (1982) composite anomaly wind field suggests a number of differences (see section 3). However, these islands are in areas of the ocean where very little ship data is available and the greater amount of ship data is during the 1970s. As Luther and Harrison (1984) have shown, the considerable amount of high frequency variability present in the wind field makes it difficult to obtain accurate monthly mean values without at least ten random observations per month; this level of sampling is hardly ever available from ships in the area of interest. In fact, RC indicate that their composite results in this area are of uncertain reliability. The major differences are that the meridional extent of the equatorial island westerlies seems to be much smaller and the island anomalies are much stronger than suggested in RC, and there is little indication of the persistent systematic off-equatorial meridional anomalies suggested in RC. Our knowledge of the large-scale tropical anomaly patterns associated with El Niño events is obviously far from complete.

Several provocative issues are raised by these island results and deserve further attention. First, the fact that the evolution of the wind field between July 1958 and July 1959 is so very similar to that of the other events (excepting 1969) suggests that it should perhaps be considered a separate El Niño event (at least as far as the near surface atmosphere is concerned) that occurred immediately after the 1957 El Niño. That no other event has any significant anomalies by July (+1) also supports this interpretation. If this is correct, ENSO episodes do not require a period of anomalous equatorial easterly winds to precondition the Pacific and prime it for an event. Unfortunately the available ocean data base for 1957–59 is very sparse, and it is hard to describe with any confidence even the SST field for this period; almost no data on the subsurface equatorial thermal structure is available.

A second issue concerns the direction of evolution of the wind field during El Niño events. The Rasmusson and Carpenter (1982) composites have been interpreted to suggest that the SST anomaly during year (0) expands westward out along the equator and intensifies in summer–fall of year (0). According to the simple atmospheric model response to imposed atmospheric heating found in Gill (1980) and Zebiak (1982), westerly anomalies should be maximum in the western part

of the heating anomaly. Of course the relation between SST anomaly and atmospheric heating is not simple, or even well known, but Zebiak (1985) finds that a related model for the forced response of the atmosphere over the tropical Pacific predicts westerly wind anomalies over the western part of a warm SST anomaly near and/or east of the date line. If the warm anomaly in fact expands westward along the equator and the heating is roughly proportional to the SST anomaly, the evolution of the near-equatorial surface wind anomalies observed to occur here is inconsistent with these model predictions.

A third issue involves the very narrow meridional scale of the surface zonal wind anomalies observed both in individual El Niño events and in the composites. A meridional scale of 2 or 3 degrees of latitude for an anomaly centered on the equator or slightly south of the equator is small compared to the natural free scale for atmospheric waves (typically  $\sim 10^\circ$  of latitude; see e.g., Zebiak, 1982). If the westerly anomaly scale is set by the scale of an atmospheric forcing, either the forcing is much narrower meridionally than has been thought previously, or the character of the interactions between the winds in the planetary boundary layer and higher up is quite special. At 850 mb the meridional scale appears to be much larger (e.g., Harrison and Gutzler, 1986).

Another issue revolves around the transition from a pattern of equatorially centered and trapped westerly anomalies to a comparably narrow pattern of westerly anomalies centered perhaps  $5^\circ\text{S}$  of the equator. Does a presumably narrow band of equatorial heating simply shift southward 5 deg, and disappear the following month? It would be very desirable to see if detailed analysis of the outgoing longwave radiation data can shed any light on the mechanism of the shift. Because there can be a lapse of one or more months between the period of strong equatorially trapped westerlies and the jump to southward displaced westerlies, it seems reasonable to assume that distinct physical situations pertain to the two conditions. Again it is unfortunate that there are no data available on the distribution of atmospheric heating east of these islands.

One of the disappointments of this analysis is that there is so little clear signal associated with the early months of the year (0), during which SST first warms off the South American coast. At least between  $170^\circ\text{E}$  and  $160^\circ\text{W}$  and within  $10^\circ$  of the equator, no clear pattern of wind or wind anomalies is found. Either these islands are most unserendipitously located and the early year (0) signals are elsewhere or the signals are simply inappropriate to emerge from a study of monthly means for just a few El Niño events. A recent study of wind variations through the troposphere between Canton and the eastern Indian Ocean by Gutzler and Harrison (1987) also found no clear signal in the December (–1) through February (0) season, and very weak signal in this part of the ocean in the March (0) through May (0) season. The results of Luther et al.

(1983) and Barnett (1983) suggest that precursive signal may exist further west. We shall pursue this issue elsewhere.

The evolution of the surface wind field during El Niño periods and its relationships with the evolution of SST remain a crucial aspect of the El Niño–Southern Oscillation phenomenon that is poorly understood. Hopefully it will be possible soon to understand the mechanisms that underlie the very clear and distinctive patterns of wind change documented here in the central Pacific, and to move from there to a more complete understanding of the El Niño–Southern Oscillation phenomenon.

*Acknowledgments.* D. E. Harrison is supported by the EPOCS and TOGA programs of NOAA, and this study was initiated under NSF Grant OCE-83-01787 to Massachusetts Institute of Technology. The programming assistance of Mark Terman and discussions with E. S. Sarachik, D. Gutzler and M. Wallace are also gratefully acknowledged. The raw island data used here were made available through the kindness of the New Zealand Meteorological Service, and particularly Mr. J. D. W. Hessel; these raw data were keypunched and edited under the care of Dr. D. Luther.

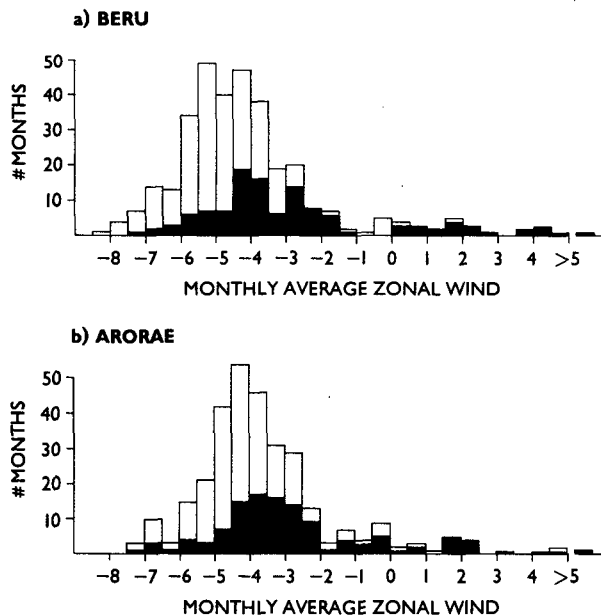


FIG. A1. Frequency distributions of monthly mean winds at Beru and Arorae islands. Shaded distributions correspond to El Niño period winds. Westerly outliers almost all correspond to El Niño periods, and there are no comparably anomalous easterly outliers.

## APPENDIX

### Frequency Distribution of Near-Equatorial Island Monthly Mean Winds

To support the statement made in the text concerning the absence of any clear “anti-El Niño” counterpart to the El Niño period zonal winds, consider Fig. A1, which presents frequency distributions of monthly average zonal wind for Beru ( $1^{\circ}\text{S}$ ,  $176^{\circ}\text{E}$ ) and Arorae ( $3^{\circ}\text{S}$ ,  $177^{\circ}\text{E}$ ) islands. The distributions for the extended group of El Niño events (see text) and for all the data between 1953 and 1980 are indicated. El Niño periods have quite an extreme distribution, with a number of examples of westerly wind widely displaced from the main body of the distribution. No corresponding easterly outliers are found for the complete zonal wind distribution.

## REFERENCES

- Barnett, T. P., 1983: Interaction of the monsoon and Pacific trade wind system at interannual time scales. Part I: The equatorial band. *Mon. Wea. Rev.*, **111**, 756–773.
- Busalacchi, A. J., and J. J. O’Brien, 1981: Interannual variability of the equatorial Pacific in the 1960s. *J. Geophys. Res.*, **86**, 10 901–10 907.
- Gill, A. E., 1980: Some simple solutions for heat-induced tropical circulations. *Quart. J. Roy. Meteor. Soc.*, **106**, 447–462.
- Goldenberg, S. B., and J. J. O’Brien, 1981: Time and space variability of tropical Pacific wind stress. *Mon. Wea. Rev.*, **109**, 1190–1207.
- Gutzler, D., and D. E. Harrison, 1987: The structure and evolution of seasonal wind anomalies over the near-equatorial eastern Indian and Western Pacific oceans. *Mon. Wea. Rev.*, **115**, 169–192.
- Harrison, D. E., and D. Gutzler, 1986: Variability of monthly averaged surface and 850 mb winds at tropical Pacific islands. *Mon. Wea. Rev.*, **114**, 285–294.
- Luther, D. S., and D. E. Harrison, 1984: Observing long-period fluctuations of surface winds in the tropical Pacific: Initial results from island data. *Mon. Wea. Rev.*, **112**, 285–302.
- , —, and R. Knox, 1983: Zonal winds in the central equatorial Pacific and the onset of El Niño. *Science*, **222**, 327–330.
- Rasmusson, E. M., and T. H. Carpenter, 1982: Variations in tropical sea surface temperature and surface wind fields associated with the Southern Oscillation/El Niño. *Mon. Wea. Rev.*, **110**, 354–384.
- Wyrki, K., and G. Meyers, 1975: The trade wind field over the Pacific Ocean. Part 2: Bimonthly fields. Hawaii Institute of Geophysics, Rep. HIB-75-2, University of Hawaii, Honolulu.
- Zebiak, S. E., 1982: A simple atmospheric model of relevance to El Niño. *J. Atmos. Sci.*, **39**, 2017–2027.
- , 1985: Tropical ocean–atmosphere interaction and the El Niño/Southern Oscillation phenomenon. Ph.D. thesis, Center for Meteorology and Physical Oceanography, Massachusetts Institute of Technology.